

Role of protein kinase C δ in ER stress and apoptosis induced by oxidized LDL in human vascular smooth muscle cells

P Larroque-Cardoso^{1,2,5}, A Swiader^{1,2,5}, C Ingueneau^{1,2}, A Nègre-Salvayre^{1,2}, M Elbaz^{1,2,3}, ME Reyland⁴, R Salvayre^{1,2} and C Vindis^{*,1,2}

During atherogenesis, excess amounts of low-density lipoproteins (LDL) accumulate in the subendothelial space where they undergo oxidative modifications. Oxidized LDL (oxLDL) alter the fragile balance between survival and death of vascular smooth muscle cells (VSMC) thereby leading to plaque instability and finally to atherothrombotic events. As protein kinase C δ (PKC δ) is pro-apoptotic in many cell types, we investigated its potential role in the regulation of VSMC apoptosis induced by oxLDL. We found that human VSMC silenced for PKC δ exhibited a protection towards oxLDL-induced apoptosis. OxLDL triggered the activation of PKC δ as shown by its phosphorylation and nuclear translocation. PKC δ activation was dependent on the reactive oxygen species generated by oxLDL. Moreover, we demonstrated that PKC δ participates in oxLDL-induced endoplasmic reticulum (ER) stress-dependent apoptotic signaling mainly through the IRE1 α /JNK pathway. Finally, the role of PKC δ in the development of atherosclerosis was supported by immunohistological analyses showing the colocalization of activated PKC δ with ER stress and lipid peroxidation markers in human atherosclerotic lesions. These findings highlight a role for PKC δ as a key regulator of oxLDL-induced ER stress-mediated apoptosis in VSMC, which may contribute to atherosclerotic plaque instability and rupture.

Cell Death and Disease (2013) 4, e520; doi:10.1038/cddis.2013.47; published online 28 February 2013

Subject Category: Experimental Medicine

Atherosclerosis is a slow degenerative process and is the underlying cause of heart attacks, strokes, and peripheral artery diseases in humans. This complex disorder is characterized by the focal accumulation of lipids and the remodeling of the arterial wall, leading to the formation of the atherosclerotic plaque. Modified lipoproteins, specially oxidized low-density lipoproteins (oxLDL), are present within atheroma plaques, and are thought to play a role in atherogenesis.¹ OxLDL exhibit a variety of atherogenic properties, by inducing foam cell formation, inflammatory response, cell proliferation, at low concentration, and apoptosis at higher concentration.^{2,3} The balance between aberrant proliferation and apoptosis is responsible for mediating intense changes in the development of atherosclerosis. Apoptosis of vascular smooth muscle cells (VSMC) increases as atherosclerotic plaques develop and is sufficient to induce features of plaque vulnerability in atherosclerosis.⁴ Overall, loss of VSMC is detrimental for plaque stability and increases the risk of thrombotic events.

The apoptotic signaling triggered by oxLDL is mediated through a complex sequence of signaling events that lead to activation of caspase-dependent or caspase-independent

apoptotic pathways. We previously reported that treatment of human VSMC with oxLDL induced a sustained rise of cytosolic calcium, leading to the activation of the intrinsic mitochondrial apoptotic pathway.^{5,6} More recently, we showed in human vascular endothelial cells an interaction between the deregulation of cytosolic calcium and the endoplasmic reticulum (ER) stress in triggering the apoptotic response induced by oxLDL.⁷ ER plays an essential role in sensing cellular stress (i.e., accumulation of misfolded proteins, potential redox or calcium deregulation) as it rapidly detects changes in cell homeostasis, and responds by eliciting UPR (unfolded protein response) via the activation of ER transmembrane sensors, PERK (double-stranded RNA-dependent protein kinase (PKR)-like ER kinase), IRE1 α (inositol-requiring 1 α) and ATF6 (activating transcription factor 6). The UPR results in a temporary downregulation of protein translation, an upregulation of ER chaperones and folding machinery, and the expression and activation of ER-associated degradation (ERAD).⁸ Prolonged ER stress switches towards apoptotic cell death via the activation of downstream signals like CHOP (C/EBP homologous protein), JNK and members of the Bcl-2 family.^{9,10} Our previous data¹¹ and

¹INSERM UMR 1048/I2MC, Toulouse, France; ²Université Toulouse 3, PRES, Toulouse, France; ³Department of Cardiology, CHU Rangueil, Toulouse, France and ⁴Department of Craniofacial Biology, Anschutz Medical Campus School of Dental Medicine, University of Colorado Denver, Aurora, CO 80045, USA

*Corresponding author: C Vindis, Vascular Biology, Team 10, INSERM UMR 1048/I2MC—Team, Atherosclerosis—Graft Arteriosclerosis, CHU Rangueil, 1 Avenue Jean Poulhès—BP84225, Toulouse, Cedex 4 31432, France. Tel: +33 561 32 2705; Fax: +33 561 32 2084; E-mail: cecile.vindis@inserm.fr

⁵These two authors contributed equally to this work.

Keywords: PKC δ ; oxidized low-density lipoproteins; apoptosis; ER stress; vascular smooth muscle cells

Abbreviations: PKC δ , protein kinase C δ ; oxLDL, oxidized low-density lipoprotein; ER stress, endoplasmic reticulum stress; VSMC, vascular smooth muscle cells; UPR, unfolded protein response; ROS, reactive oxygen species

Received 26.7.12; revised 07.1.13; accepted 15.1.13; Edited by Y Shi

those from Myoishi *et al.*¹² demonstrated that ER stress markers are present in human advanced atherosclerotic lesions thus raising the question of the possible role of ER stress in the stability/instability of atherosclerotic plaques, since this adaptive response may influence the fate of cells to survive or die.

Protein kinase C δ (PKC δ), a member of the PKC family of serine–threonine kinases, is known to be a critical pro-apoptotic signal in many cell types.¹³ More particularly, PKC δ -deficient mice develop exacerbated intimal hyperplasia associated with diminished SMC apoptosis in vein grafts¹⁴ and carotid ligation models,¹⁵ indicating that PKC δ is an important regulator of SMC apoptosis after vascular injury. Recently, it has been shown that PKC δ plays a crucial role in the propagation of TNF α -induced ER stress-mediated JNK activation and CHOP/GADD53 induction.¹⁶ Hitherto, whether PKC δ contributes to oxLDL-induced vascular SMC apoptosis and ER stress is not known.

Here, we investigated the possible involvement of PKC δ in the apoptotic signaling pathway triggered by oxLDL and its role in the transmission of the pro-apoptotic signal of the ER stress in human VSMC. We found that oxLDL mediate PKC δ activation through reactive oxygen species (ROS) production and that PKC δ plays a crucial role in the regulation of oxLDL-induced apoptosis mainly through the IRE1 α /JNK pathway of ER stress. Importantly, we provided evidence that activated PKC δ is colocalized with ER stress and lipid peroxidation markers in human atherosclerotic lesions.

Results

siRNA-mediated suppression of PKC δ expression reduces oxLDL-induced human vascular smooth muscle apoptosis. We first investigated the involvement of PKC δ in the apoptosis of human vascular smooth muscle (hVSMC) cells treated with oxLDL. The expression of PKC δ was silenced by small interfering RNA (siRNA) specific to human PKC δ As shown in Figure 1a. The inhibitory effect of siRNA on PKC δ expression was obvious 48 h after transfection and was not influenced by treatment with oxLDL. To assess whether the effect of PKC δ knockdown relates to hVSMC survival, PKC δ knockdown () and control cells were treated with oxLDL for 24 h. PKC δ knockdown cells displayed a protection towards oxLDL-induced apoptosis as demonstrated by a significant decrease in cell death (Figure 1b). The involvement of caspase-3 is supported by the protective effect of the multicaspase inhibitor z-VAD-fmk against oxLDL-induced apoptosis (Figure 1c). We also showed the release of cytochrome C from the mitochondria, which is accompanied by an increased expression of the pro-apoptotic protein Bak and a decreased expression of the pro-survival protein Bcl-2 in agreement with the data of Yang *et al.*¹⁷ (Supplementary Figure S1). The activation of caspase-3 is prevented in PKC δ knockdown cells as shown by the inhibition of its cleavage, compared with control cells (Figure 1d).

We further demonstrated the involvement of PKC δ in the apoptosis induced by oxLDL by the use of mouse embryonic fibroblasts (MEF) inactivated for PKC δ MEF PKC δ ^{-/-} that showed a strong resistance to oxLDL-induced cell death as

explored by cell viability assay, apoptotic characteristics, Bcl-2 expression, cytochrome C release and caspase-3 cleavage compared with MEF PKC δ cells (Figures 2a–e). Moreover, the central role of PKC δ in the broad regulation() of apoptosis is supported by the protection of MEF PKC δ ^{-/-} cells towards the apoptotic inducer antimycin A (Figure 2a).

The resistance to apoptosis in PKC δ ^{-/-} cells likely results from the loss of PKC δ expression, to prove that apoptosis is directly dependent on PKC δ we asked if the re-expression of PKC δ is sufficient to restore the apoptotic response induced by oxLDL.

MEF PKC δ ^{-/-} cells were transduced with adenovirus expressing either GFP (AdGFP) or a PKC δ -GFP (AdPKC δ -GFP) fusion protein (Figure 3a). As shown in Figure 3b, transduction of AdPKC δ -GFP completely re-establishes their apoptotic response to oxLDL, whereas PKC δ ^{-/-} cells transduced with AdGFP remained resistant to oxLDL-induced apoptosis. Our data clearly demonstrate that re-expression of PKC δ in PKC δ ^{-/-} cells reconstitute apoptotic potential. Altogether, our results indicate that PKC δ plays a major role in the apoptosis induced by oxLDL.

PKC δ is activated in response to oxLDL stimulation in human vascular smooth muscle.

The ability of PKC δ to activate an apoptotic program is regulated by key events such as phosphorylation on specific tyrosine residues and nuclear accumulation where it may be cleaved by caspase to generate a pro-apoptotic PKC δ catalytic fragment (δ CF).¹³ We analyzed the phosphorylation of PKC δ on tyrosine 311 because (i) this critical residue located in the catalytic domain is phosphorylated in response to apoptotic stimulus such as oxidative stress induced by hydrogen peroxide^{18,19} and because (ii) oxLDL treatment generates an oxidative stress through the production of hydrogen peroxide (H₂O₂) and superoxide anion (O₂⁻).²⁰ To examine the effect of oxLDL on PKC δ tyrosine 311 phosphorylation, hVSMC were treated with increasing concentrations of oxLDL (0–200 μ g ApoB/ml) for 5 h or with cytotoxic concentration of oxLDL (200 μ g ApoB/ml) for 1–8 h. As shown in Figure 4a, the phosphorylation level of tyrosine 311 increases with the concentration of oxLDL and with the length of time treatment being visible at 5 h stimulation. We then followed the nuclear translocation of PKC δ by two methods: cell fractionation and fluorescence microscopy. After hVSMC treatment with oxLDL, the nuclear and cytosolic fractions were separated by differential centrifugation. We found that in untreated cells, PKC δ was expressed in the cytosol and translocated to the nucleus beyond 12 h of oxLDL stimulation (Figure 4b). Using immunofluorescence microscopy, we confirmed that PKC δ was located mostly in the cytosol in untreated control cells and that oxLDL induced the translocation of PKC δ to the nucleus in about 90–95% of the cells as observed following 18 h treatment with oxLDL (Figure 4c). Collectively, these data show that oxLDL induce the activation of PKC δ to trigger hVSMC apoptosis.

ROS generated by oxLDL contribute to the activation of PKC δ . We then questioned the mechanisms involved in oxLDL-induced PKC δ activation. We previously showed that oxLDL trigger an intracellular rise in ROS in rabbit smooth muscle cells.²¹ Therefore, we investigated whether oxLDL-

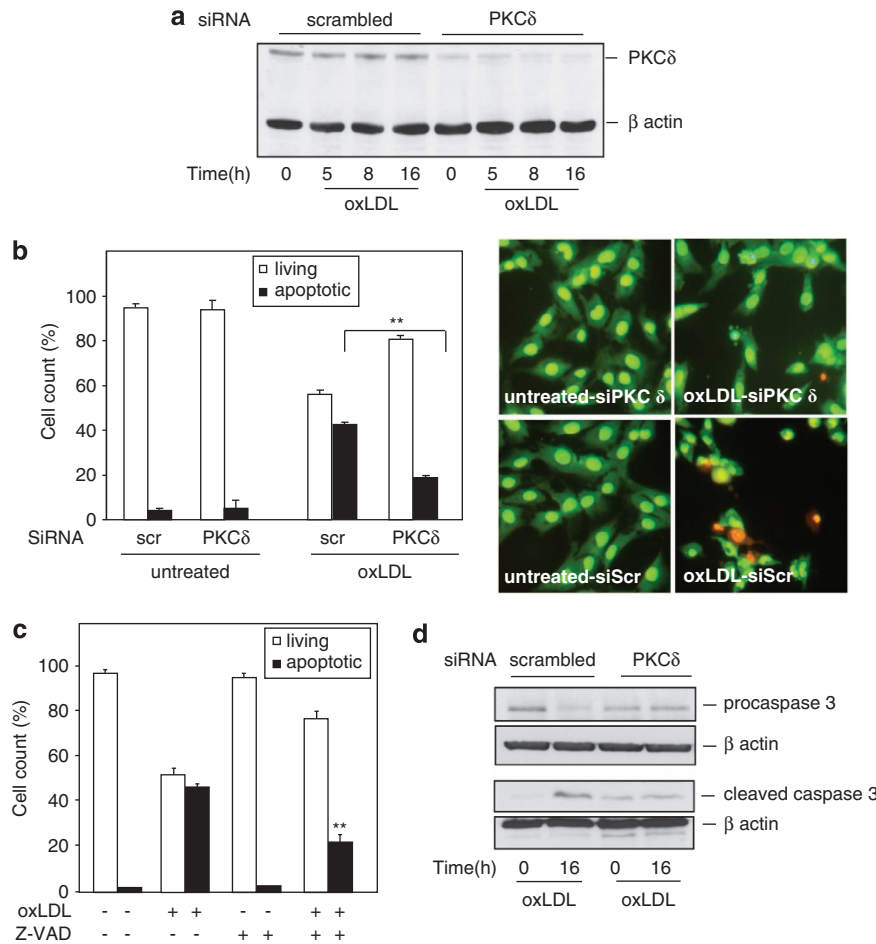


Figure 1 SiRNA silencing of PKC δ reduced oxLDL-induced apoptosis of human VSMC. (a) Representative western blot of the expression of PKC δ after siRNA silencing. Human VSMC were transfected with 100 nM scrambled siRNA or 100 nM PKC δ siRNA for 48 h as described under 'Materials and Methods.' After siRNA transfection, hVSMC were treated with oxLDL (200 μ g ApoB/ml) at the indicated times. Immunoblots were performed on cell lysates using an anti-PKC δ antibody and β -actin was used as a loading control. (b) Analysis of oxLDL-induced cell death. Human VSMC transfected with scrambled (scr) or PKC δ siRNA were incubated with oxLDL (200 μ g ApoB/ml) for 24 h and apoptotic cells were counted after staining with SYTO-13/PI as described under 'Materials and Methods.' The left graph represents the results expressed as percentage of untreated control and the mean \pm S.E.M. of four independent experiments (>200 cells were counted for each variable per experiment). ** $P < 0.01$ indicates significance (comparison between apoptotic cells from scr siRNA transfected cells + oxLDL and PKC δ siRNA transfected cells + oxLDL groups). The left panel illustrates the SYTO-13/PI labeling of human VSMC treated or not with oxLDL (200 μ g ApoB/ml, for 24 h). (c, d) Involvement of caspase-3 in oxLDL-induced apoptosis. (c) Human VSMC pretreated with z-VAD-fmk (50 μ M) were incubated with oxLDL (200 μ g ApoB/ml) for 24 h and apoptotic cells were counted after staining with SYTO-13/PI as described under 'Materials and Methods.' The graph represents the results expressed as percentage of untreated control and the mean \pm S.E.M. of four independent experiments (>200 cells were counted for each variable per experiment). ** $P < 0.01$ indicates significance (comparison between apoptotic cells from oxLDL-treated and z-VAD + oxLDL-treated groups). (d) Representative western blot of time-course analysis of procaspase-3 processing and cleaved caspase-3 generation in human VSMC transfected with scrambled or PKC δ siRNA and treated with oxLDL (200 μ g ApoB/ml, 16 h). Immunoblots representative of three independent experiments, were performed on cell lysates using anti-procaspase-3, anti-cleaved caspase-3 antibodies and β -actin was used as a loading control

induced ROS generation is involved in PKC δ tyrosine 311 phosphorylation. Incubation of hVSMC with oxLDL but not with nLDL (data not shown) resulted in a rapid increase of intracellular ROS as assessed by the rise of DCF fluorescence (Figure 5a). OxLDL-mediated ROS production is prevented by preincubation with the NADPH oxidase inhibitor 3-benzyl-7-(2-benzoxazolyl)thio-1,2,3-triazolo[4,5-d]pyrimidine (VAS2870, 10 μ M) and with the addition of a cell permeable form of the antioxidant enzyme catalase (PEG-catalase 50 U/ml). Indeed, addition of PEG-conjugated enzyme produces an increase in plasma membrane fluidity, thus enhancing cell association and uptake.²² These data suggest that NADPH oxidases play a major role in the generation of ROS by oxLDL and that H₂O₂ produced

through the dismutation of O₂⁻ might be the mediator of ROS-induced cell signaling. We further analyzed the inhibitory efficiency of VAS2870 and PEG-catalase on the tyrosine 311 phosphorylation of PKC δ . As shown in Figure 5b, both antioxidants were able to prevent oxLDL-induced PKC δ phosphorylation in hVSMC. These findings demonstrate that oxLDL generate intracellular ROS responsible for PKC δ activation. Moreover, the inhibitory effect of VAS2870 suggests that ROS production depends on the activity of NADPH oxidase in hVSMC.

The UPR is induced upon oxLDL stimulation and the activation of the ER stress-dependent IRE1/JNK pathway is dependent on PKC δ expression. It has been

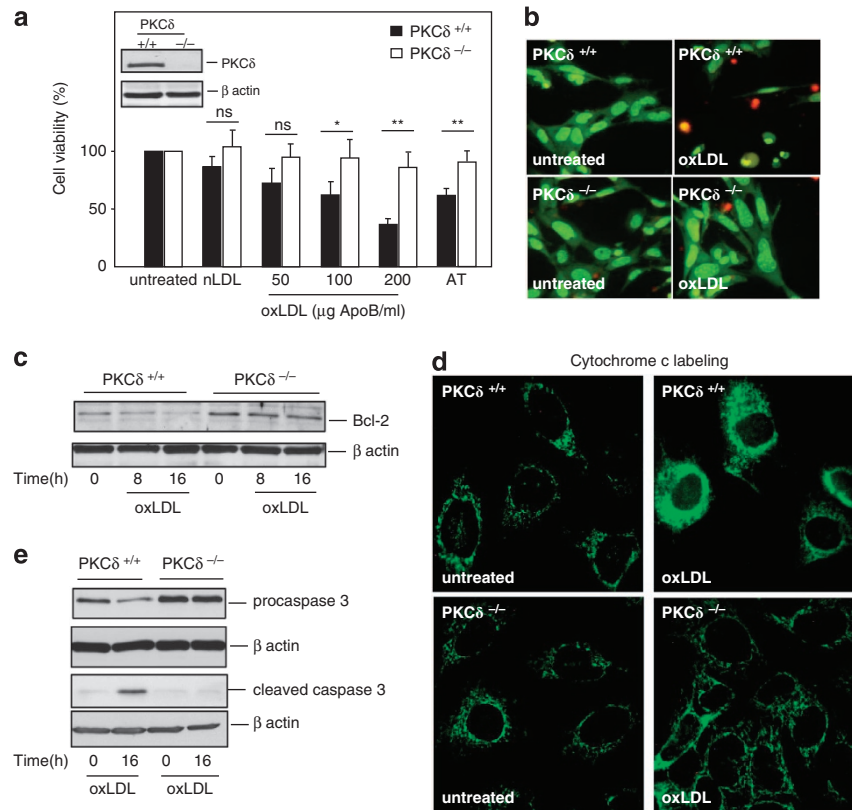


Figure 2 MEF PKC $\delta^{-/-}$ are protected from oxLDL-induced apoptosis. (a) Analysis of cell toxicity in MEF PKC $\delta^{-/-}$ and MEF wild-type (named PKC $\delta^{+/+}$) was evaluated by the MTT assay. MEF PKC δ and MEF PKC $\delta^{+/+}$ were treated with oxLDLs (50–200 μ g ApoB/ml), native LDL (nLDL, 100 μ g ApoB/ml) or antimycin A (10 μ M) for 24 h and cell toxicity was analyzed as described. Results are expressed as percentage of untreated control and represent the mean \pm S.E.M. of five separate experiments. ** $P < 0.01$ and * $P < 0.05$ indicate significance (comparison were made between PKC $\delta^{-/-}$ and PKC $\delta^{+/+}$ treated with 100 and 200 oxLDL μ g ApoB/ml or 10 μ M antimycin A), ns indicates no significance. (b) SYTO-13/PI staining of MEF PKC $\delta^{-/-}$ and MEF PKC $\delta^{+/+}$ treated or not with oxLDL (200 μ g ApoB/ml, for 24 h), the images illustrate the resistance of MEF PKC $\delta^{-/-}$ towards oxLDL-induced apoptosis. (c) Time-course analysis of Bcl-2 expression in MEF PKC $\delta^{-/-}$ and MEF PKC $\delta^{+/+}$ treated with oxLDL (200 μ g ApoB/ml). Immunoblots representative of three independent experiments were performed on cell lysates using anti-Bcl-2 antibody and β -actin was used as a loading control. (d) Immunocytochemistry experiments showing the release of the cytochrome C monitored by immunofluorescence in MEF PKC $\delta^{-/-}$ and MEF PKC $\delta^{+/+}$ treated with oxLDL (200 μ g apoB/ml) 16 h. Cells were fixed and labeled with anti-cytochrome C antibody. The results are representative of three separate experiments. (e) Representative expression blot of time-course analysis of procaspase-3 processing and cleaved caspase-3 generation in MEF PKC $\delta^{-/-}$ and MEF PKC $\delta^{+/+}$ treated with oxLDL (200 μ g ApoB/ml, 16 h). Immunoblots representative of three independent experiments were performed on cell lysates using anti-procaspase-3, anti-cleaved caspase-3 antibodies and β -actin was used as a loading control

recently shown that PKC δ participates in ER stress-induced apoptosis in mouse neuroblastoma cells.²³ To determine whether UPR is induced in hVSMC following oxLDL treatment, we investigated the activation of the three classical ER sensors: PERK, IRE1 α and ATF6. Our data showed the phosphorylation of the PERK substrate eIF2 α an increase expression of IRE1 α ²⁴ and the nuclear translocation of ATF6 upon oxLDL stimulation in hVSMC (Figures 6a and b). Because oxLDL trigger a prolonged ER stress activation, which may have a role in apoptotic cell death through IRE1 α -TRAF2-JNK pathway and CHOP expression, we checked the activation of these proapoptotic pathways in hVSMC. OxLDL elicited the activation of JNK and the expression of CHOP protein (Figure 6c), which is in agreement with our previous studies showing the contribution of these two ER stress proapoptotic mediators in oxLDL-induced human endothelial cell apoptosis.⁷ We provided further evidence for the role of the ER stress induced by oxLDL in the apoptosis of hVSMC by showing the induction of PUMA

(p53 upregulated modulator of apoptosis) and BIM (BCL-2 interacting mediator of cell death), two pro-apoptotic BH3 domain-only proteins regulated by CHOP in response to ER stress (Figure 6d).

We next explored whether PKC δ plays a role in oxLDL-induced ER stress signaling. We observed the phosphorylation of the PERK substrate eIF2 α and the nuclear translocation of ATF6 in MEF PKC $\delta^{+/+}$ and PKC $\delta^{-/-}$ cells following oxLDL treatment (Figures 7a and b). On the other side, in PKC $\delta^{+/+}$ cells oxLDL induced the expression of IRE1 α and CHOP, and JNK activation whereas PKC $\delta^{-/-}$ cells treated with oxLDL displayed neither increased expression of IRE1 α nor JNK activation but showed an increased expression of CHOP (Figures 7a and c).

We then asked whether PKC δ was necessary for the induction of the UPR. MEF PKC $\delta^{+/+}$ and PKC δ cells were stimulated by thapsigargin a potent inducer of ER stress. The activation of the UPR and the ER stress proapoptotic mediators was observed in cells expressing or not PKC δ

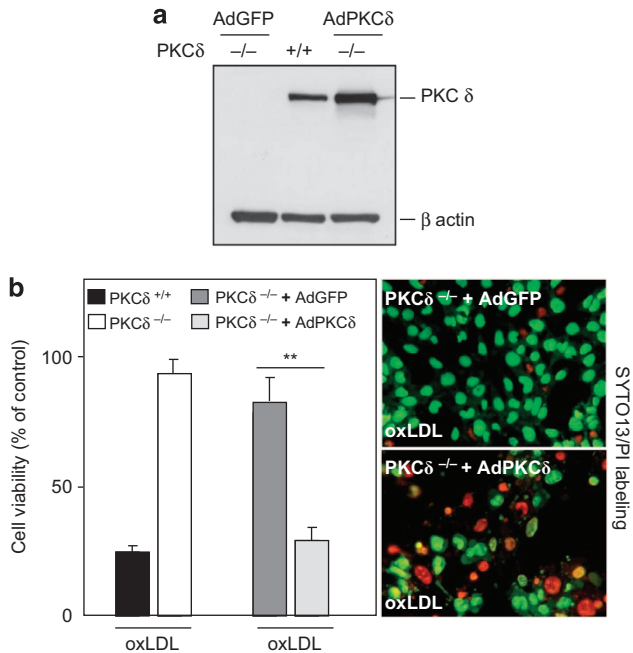


Figure 3 Re-expression of PKC δ -GFP in MEF PKC δ ^{-/-} cells reconstitutes apoptotic potential. **(a)** Western blot analysis of re-expression of PKC δ in MEF PKC δ ^{-/-} compared with MEF PKC δ ^{+/+}. MEF PKC δ ^{-/-} were infected with adenovirus GFP (AdGFP) or a PKC δ -GFP (AdPKC δ -GFP) fusion protein for 24 h. Immunoblots were performed on cell lysates using anti-PKC δ and β -actin was used as a loading control. **(b)** Analysis of cell toxicity in MEF PKC δ ^{-/-} expressing AdPKC δ -GFP or AdGFP fusion protein was evaluated by the MTT assay. MEF PKC δ ^{-/-} infected with adenovirus GFP (AdGFP) or a PKC δ -GFP (AdPKC δ -GFP) fusion protein for 24 h. Cells were treated or not with oxLDLs (200 μ g ApoB/ml) for 24 h and cell toxicity (left panel) was analyzed as described. Results are expressed as percentage of untreated control and represent the mean \pm S.E.M. of four separate experiments. ** P < 0.01 indicate significance (comparison were made between PKC δ ^{-/-} + AdGFP and PKC δ ^{-/-} + AdPKC δ -GFP treated with oxLDL). SYTO-13/PI labeling (right panel) of PKC δ ^{-/-} + AdGFP and PKC δ ^{-/-} + AdPKC δ -GFP treated with oxLDL (200 μ g ApoB/ml, for 24 h), the images illustrate the restoration of the apoptotic potential of MEF PKC δ ^{-/-} expressing AdPKC δ -GFP. Cells treated with oxLDL showed chromatin condensation and appearance of apoptotic bodies, because of the brightness of SYTO-13, GFP fluorescence is not apparent

(Supplementary Figure S2), indicating that PKC δ does not globally regulate the ER stress.

Therefore, our results demonstrated for the first time that PKC δ participates in oxLDL-induced ER stress-dependent apoptotic signaling mainly through the IRE1/JNK pathway.

Activated PKC δ colocalized with ER stress and oxidative markers in human atherosclerotic lesions. Since oxLDL and oxidized lipids are found in atherosclerotic lesions, we investigated whether PKC δ phosphorylated on tyrosine 311 is expressed in human atherosclerotic lesions of carotid endarterectomy. Immunostaining of phosphorylated PKC δ was strongly positive in the necrotic core of advanced atherosclerotic lesions compared with normal mammary artery where phosphorylated PKC δ was not detected (Figure 8). Interestingly, the staining of UPR markers with KDEL (Lys-Asp-Glu-Leu) antibody that recognizes both ER chaperones GRP78 and GRP94, was increased in advanced

lesions and colocalized with PKC δ phosphorylated and the lipid peroxidation marker 4-hydroxynonenal (4-HNE). In normal artery, there was no KDEL or 4-HNE positivity. Furthermore, we confirmed that KDEL-, 4-HNE- and activated PKC δ -positive cells were foams cells (SMC and macrophages) of the necrotic core as shown by immunostaining of serial sections with anti-CD68 antibody. These results support our *in vitro* data and strongly suggest that PKC δ and ER stress may be activated by oxidized lipids within the atherosclerotic lesions.

Discussion

OxLDL-induced apoptosis of vascular cells may contribute to the erosion and instability of atherosclerotic plaques, thereby increasing the risk of subsequent thrombotic events. In this study, we identified a novel regulatory pathway in oxLDL-induced apoptosis of VSMC. We report for the first time that PKC δ is activated by oxLDL in human VSMC and contributes to oxLDL-induced ER stress-dependent apoptotic signaling through the IRE1 α /JNK pathway.

The function of PKC δ depends on the cell type and specific stimulus but currently a large number of studies are consistent with the central role of PKC δ in the regulation of cell apoptosis in response to various apoptotic stimuli.²⁵ We showed that knockdown of PKC δ expression significantly reduces the effect of oxLDL-induced apoptosis in primary human VSMC and reintroduction of PKC δ into PKC δ knockout cells restores their apoptotic capacity, indicating that PKC δ is sufficient to specifically control the ability of the cells to undergo apoptosis. In addition, the modulation of the expression of pro-apoptotic and pro-survival members of the Bcl-2 family and, the reduced release of cytochrome C in PKC δ knockout cells suggests that PKC δ plays a central role in the mitochondria-dependent apoptotic pathway triggered by oxLDL. Altogether our findings corroborate previous results showing that forced higher expression in normal VSMC increased their apoptotic responses to the H₂O₂.¹⁵ However, it has been demonstrated that SMC isolated from PKC δ knockout mice displayed decreased proliferation compared with wild-type SMC,²⁶ thus, suggesting that PKC δ exhibits contrasting roles in cell death and cell proliferation. In our experimental conditions, we did not observe such modification in cell viability and cell number in human VSMC knockdown for PKC δ , therefore, supporting that the proapoptotic function of PKC δ depends on the biological context.

PKC δ is activated by a large array of stimuli including mechanical stress, pro-inflammatory cytokines and oxidative stress, which are known to be associated with vascular remodeling and atherogenesis. The generation of ROS induced by oxLDL raises the question regarding how PKC δ is activated, which may include binding of second messenger diacylglycerol, phosphorylation, membrane translocation and proteolysis. One of the key event involved in the transduction of a death signal to PKC δ is the phosphorylation of PKC δ on tyrosine residues. In this study, we provided evidence that the rise in intracellular ROS triggered the phosphorylation of the tyrosine 311 residue of PKC δ which have been linked to increased kinase activity and apoptosis in cells treated with H₂O₂.¹⁸ The inhibitory effect of VAS2870, a well-validated

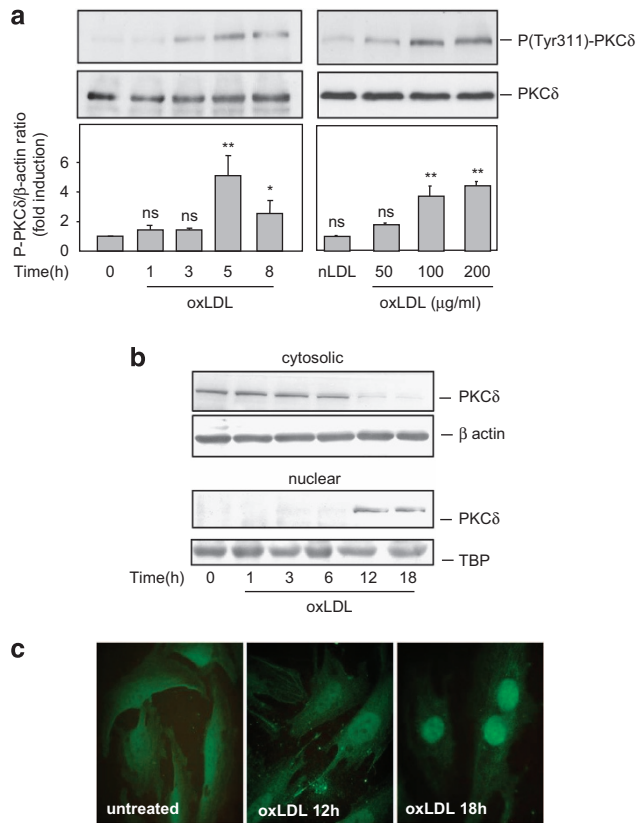


Figure 4 OxLDL induce PKC δ activation through tyrosine 311 phosphorylation and nuclear translocation in human VSMC. (a) Time-course analysis of PKC δ phosphorylation in human VSMC treated with oxLDL (200 μ g ApoB/ml). Western blot experiments were performed on total protein extracts using anti-phosphotyrosine 311 PKC δ antibody and β -actin expression was used as loading control. The graph represents values of phosphotyrosine 311 PKC δ band intensity after normalization for total PKC δ by densitometry, * P <0.05 and ** P <0.01 indicate significance (comparison between untreated cells and oxLDL 5 h and between untreated cells and oxLDL 8 h), ns indicates no significance. Blots are representative of four independent experiments. (b) Time-course analysis showing nuclear translocation of PKC δ in human VSMC treated with oxLDL (200 μ g ApoB/ml). Immunoblots were performed on cell lysates and analyzed for the presence of PKC δ after nuclear and cytosolic fractionation as described under 'Materials and Methods.' TBP (TATA-binding protein, nuclear marker) and β -actin (cytosolic marker) were also used as a loading control. Blots are representative of three independent experiments. (c) Immunocytochemistry experiments showing the nuclear translocation of PKC δ monitored by immunofluorescence in human VSMC treated with oxLDL (200 μ g ApoB/ml) for 12 or 18 h. Cells were fixed and labeled with anti-PKC δ antibody. The results are representative of three separate experiments

specific inhibitor of NADPH oxidase (NOX),²⁷ on oxLDL-induced ROS production and PKC δ tyrosine 311 phosphorylation raises the question of the enzymatic sources of ROS. Our data are consistent with the work of Stielow who showed that the VAS2870 inhibited²⁸ oxLDL-induced ROS production in HUVEC. Moreover, the antioxidant enzyme catalase exerts the same inhibitory effect as VAS2870, which also supports a potential role of H₂O₂ generated by oxLDL treatment on PKC δ activation.

The main substrates of PKC δ in apoptotic cells are nuclear proteins and it has been shown that PKC δ translocates from the cytoplasm to the nucleus in response to specific apoptotic

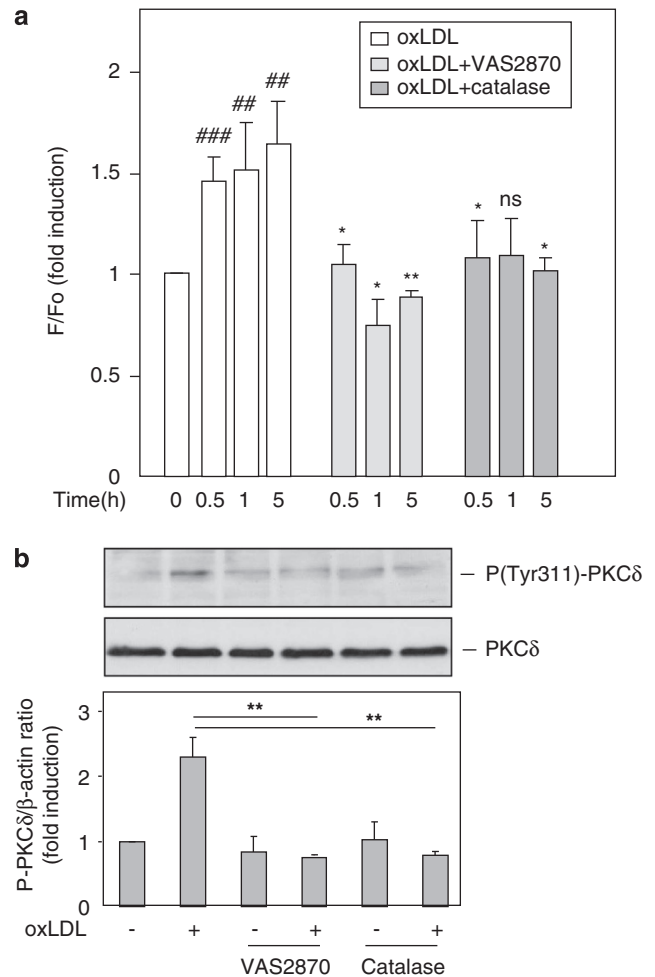


Figure 5 ROS generation mediated by oxLDL is involved in the activation of PKC δ . (a) Measurement of intracellular ROS production using the free radical sensor: H₂DCFDA (6-carboxy-2',7'-dichlorodihydrofluorescein diacetate). Human VSMC were pretreated with the NADPH inhibitor (VAS-2870, 10 μ M) or with PEG-catalase (50 UI/ml) for 1 h, then incubated with oxLDL (200 μ g apoB/ml) for 0.5, 1 and 5 h. The variation of intracellular ROS was detected by fluorescence intensity using the free radical sensor: 6-carboxy-2',7'-dichlorodihydrofluorescein diacetate as described under 'Materials and Methods.' Results were normalized on protein levels and expressed in ratio to untreated control. The data are expressed as mean \pm S.E.M. of five separate experiments * or # P <0.05; ** or ## P <0.01 indicate significance, (# comparison between untreated cells and oxLDL-treated cells, * comparison between oxLDL-treated cells and oxLDL + VAS2870, between oxLDL-treated cells and oxLDL + catalase). ns indicates no significance. (b) Analysis of oxLDL-induced PKC δ phosphorylation in human VSMC pretreated with NADPH inhibitor (VAS-2870, 10 μ M) or with PEG-catalase (50 UI/ml). Western blot experiments were performed on total protein extracts treated with oxLDL (200 μ g ApoB/ml) for 8 h, using anti-phosphotyrosine 311 PKC δ antibody and total PKC δ expression was used as loading control. The graph represents values of phosphotyrosine 311 PKC δ band intensity after normalization for total PKC δ by densitometry, ** P <0.01 indicates significance (comparison between oxLDL and oxLDL + VAS2870, between oxLDL and oxLDL + catalase). Blots are representative of three independent experiments

stimuli.²⁹ Indeed, a nuclear localization sequence (NLS) has been defined in PKC δ that is required for its ability to induce apoptosis.³⁰ As we observed a nuclear localization of PKC δ following oxLDL stimulation, we can hypothesize that oxLDL through the production of ROS, may induce post-translational

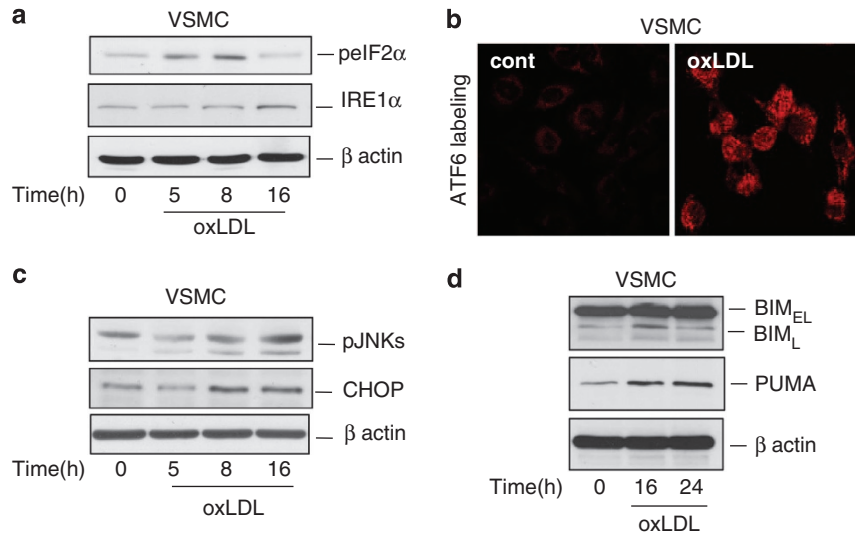


Figure 6 OxLDL trigger UPR and pro-apoptotic ER stress pathways in human VSMC. Time course of ER stress sensors activation in human VSMC treated with oxLDL (200 μ g ApoB/ml). (a) Western blot experiments were performed on total protein extracts, cell lysates were assessed for phospho-eIF2 α and IRE1 α expression. β -Actin was used as protein loading control. Blots are representative of three independent experiments. (b) Immunocytochemistry experiments show the cytoplasmic and nuclear translocation of ATF6 in human VSMC treated with oxLDL (200 μ g ApoB/ml) for 16 h. These data are representative of three separate experiments. (c, d) Time course of the ER stress pro-apoptotic mediators activation in human VSMC treated with oxLDL (200 μ g ApoB/ml). Western blot experiments were performed on total protein extracts, cell lysates were assessed for phospho-JNK, CHOP, BIM and PUMA expression. β -Actin was used as protein loading control. Blots are representative of three independent experiments

modifications in PKC δ , which allow its translocation into the nucleus. Although in some systems, apoptotic cell death is associated with caspase-3-dependent cleavage of PKC δ , we did not observe any formation of the catalytically active fragment of PKC δ in our cellular model following oxLDL treatment. Nevertheless, our results are consistent with other reports showing lack of proteolytic cleavage of PKC δ in H₂O₂-rendered apoptotic CHO cells¹⁸ or in phorbol ester-induced apoptosis in prostate cancer cells.³¹

In agreement with our previous data reporting that oxLDL induced UPR and triggered ER stress-dependent apoptosis in human endothelial cells,^{7,11} the current study demonstrated the activation of UPR sensors/ER stress in human VSMC exposed to oxLDL. The cellular response to a prolonged and excessive ER stress includes the activation of signaling pathways, which lead to apoptosis as supported by the increased expression of the proapoptotic factor CHOP/GADD53 and its targets BIM and PUMA, and the activation of the IRE1/JNK pathway in oxLDL-stimulated VSMC. To go further on the mechanisms mediating the apoptotic effect of PKC δ , we examined the potential link between ER stress and PKC δ . Interestingly, we found that PKC δ participates in oxLDL-induced ER stress-dependent apoptotic signaling mainly through the IRE1 α /JNK pathway. Indeed, we observed that in PKC δ ^{-/-} cells, oxLDL induced PERK activation, ATF6 nuclear translocation and CHOP induction but not IRE1 α /JNK activation, which is consistent with previous report showing that inhibition of PKC δ reduces ER stress-induced JNK activation in Neuro2a cells.²³ However, the regulatory role of PKC δ on ER stress is dependent on the signaling pathway triggered by the stimuli as thapsigargin induced UPR in cells expressing or not PKC δ , thus, indicating that PKC δ does not globally regulate ER stress.

The physiological importance of PKC δ in the development of atherosclerotic lesions is evidenced by our immunohistological analyses as we observed the expression of tyrosine 311 phosphorylated PKC δ in advanced human atherosclerotic lesions. Interestingly, the expression of phosphorylated PKC δ colocalized in atherosclerotic areas containing 4-HNE adducts and ER stress marker such as KDEL-positive cells, thus, suggesting that oxLDL through lipid peroxidation derivatives may locally contribute to trigger PKC δ activation and ER stress. These findings indicate that a similar activation mechanism of PKC δ such as we described in human VSMC exists in the atherosclerotic lesion. Moreover, our results corroborate the work of Yamanouchi *et al.*¹⁵ that showed a robust expression of PKC δ in apoptotic cells of human restenotic lesions.

Finally, our study identify for the first time PKC δ as a major regulator of oxLDL-induced apoptosis in VSMC, we also provide evidence that ROS generated by oxLDL are responsible for PKC δ activation. Furthermore, the involvement of PKC δ in the transmission of ER stress-dependent apoptotic signaling mainly through the IRE1 α /JNK pathway, points out that PKC δ is involved in the fine tuning of apoptosis and raises the question of its role in the stability of atherosclerotic plaque.

Materials and Methods

Reagents. Cell culture reagents were from Invitrogen Life Technologies (Saint Aubin, France). SYTO-13, propidium iodide and 6-carboxy-2',7'-dichlorodihydrofluorescein diacetate (H₂DCFDA) were from Molecular Probes (Invitrogen). VAS2870 was from Enzo Life Sciences (Villeurbanne, France), PEG-Catalase and 3-(4,5 dimethylthiazol-2-yl)-2,5-diphenyltetrazolium bromide (MTT), antimycin A from Sigma-Aldrich (Lyon, France). z-VAD-FMK was from R&D Systems Europe (Lille, France). Thapsigargin is from Calbiochem (Millipore, Saint-Quentin-en-Yvelines, France). Following antibodies were used: anti-phospho-PKC δ , anti-IRE1 α , anti-phospho-eIF2 α , anti-phospho-JNK, anti-CHOP, anti-caspase-3,

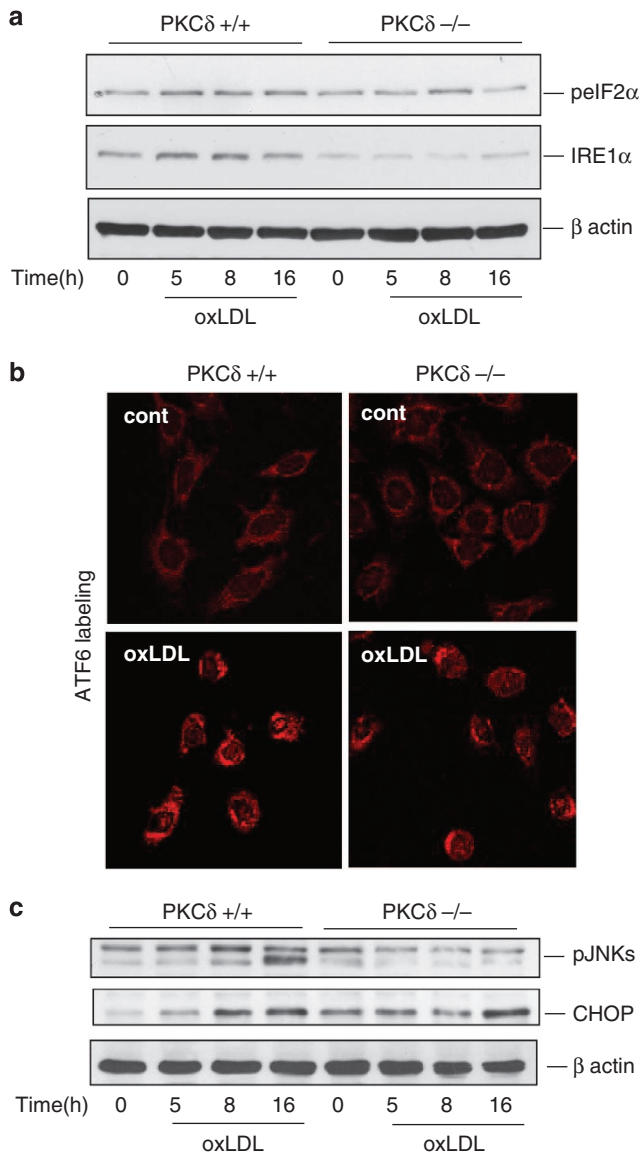


Figure 7 PKC δ is involved in the activation of the pro-apoptotic ER stress IRE1/JNK pathway but not in CHOP activation. Time course of ER stress sensors activation in MEF PKC δ ^{-/-} and MEF PKC δ ^{+/+} treated with oxLDL (200 μ g ApoB/ml). (a) Western blot experiments were performed on total protein extracts, cell lysates were assessed for phospho-eIF2 α and IRE1 α expression. β -Actin was used as protein loading control. Blots are representative of three independent experiments. (b) Immunocytochemistry experiments show the cytoplasmic and nuclear translocation of ATF6 in MEF PKC δ ^{-/-} and MEF PKC δ ^{+/+} treated with oxLDL (200 μ g ApoB/ml) for 16 h. These data are representative of three separate experiments. (c) Time course of the ER stress proapoptotic mediators activation in MEF PKC δ ^{-/-} and MEF PKC δ ^{+/+} treated with oxLDL (200 μ g ApoB/ml). Western blot experiments were performed on total protein extracts, cell lysates were assessed for phospho-JNK and CHOP expression. β -Actin was used as protein loading control. Blots are representative of three independent experiments

anti-cleaved caspase-3, anti-Bak, anti-Bim and anti-PUMA were from Cell Signaling Technology (Ozyme, Saint-Quentin-en-Yvelines, France), anti-ATF6 and anti-KDEL from Santa Cruz Biotechnology (Clinisciences, Nanterre, France), anti-cytochrome C from BD Biosciences (Le Pont de Claix, France), monoclonal anti- β -actin and anti- α -actin from Sigma-Aldrich), anti-4-HNE-adducts from Oxis Int (Foster City, CA, USA) and anti-CD68 was from NeoMarkers (Lab Vision, Fremont, CA, USA). Secondary antibodies anti-mouse and anti-rabbit were from

Santa Cruz Biotechnology and Alexa fluor 488 was from Molecular Probes (Invitrogen). The ECL chemoluminescence kit was from Amersham Pharmacia (GE Healthcare, Ramonville Saint Agne, France). Hiperfect transfection reagent was from Qiagen (Les Ulis, France).

Cell culture. Human primary VSMC were obtained from human mesenteric arteries at postmortem examinations. All experiments were conformed to the declaration of Helsinki in compliance with French legislation and written informed consent was obtained from patients for the use of surgery residual tissue for research. Briefly, the arteries were cut longitudinally and small pieces of the media were carefully stripped from the vessel wall and cultured. Within 1–2 weeks, SMC migrated from the explants; they were capable of being passaged 3 weeks after the first appearance of cells. They were identified as VSMC by their characteristic hill-and-valley growth pattern and immunohistochemistry for VSMC-specific α -actin. The primary cultured human VSMC were used to generate an immortalized cell line by using SV40T antigen, SV40T-expressing human VSMC retain expression of contractile phenotype markers including smooth muscle α -actin and smMHC to passage 10 and higher as we previously described.³² For all experiments, passage 7–17 SV40T-expressing human VSMC cultures were used. The cultures were maintained in Dulbecco's modified Eagle's medium (DMEM) supplemented with 10% fetal calf serum at 37 °C in a humidified, 5% CO₂/95% air atmosphere. MEF from PKC δ ^{-/-} mice and wild-type MEF were a generous gift from Pr. Mary E Reyland (University of Colorado Denver, USA).³³ MEF PKC δ ^{-/-} and WT were maintained in DMEM supplemented with 10% fetal calf serum at 37 °C in a humidified, 5% CO₂/95% air atmosphere.

Adenovirus expression in MEF PKC δ ^{-/-}. The generation and the use of Ad PKC δ -GFP and AdGFP have been described previously.³³ MEF PKC δ ^{-/-} were infected with Ad PKC δ -GFP or AdGFP at a multiplicity (focus forming units/cell) of 100. Cells were infected in serum-free DMEM overnight after which the virus containing medium was removed and replaced with normal medium. Infection was allowed to proceed for 24 h before stimulation with oxidized LDL.

LDL isolation and mild oxidation. LDL from human pooled sera were prepared by ultracentrifugation, dialyzed against PBS containing 100 μ M EDTA. LDL were mildly oxidized by UV-C + copper/EDTA (5 μ M) (oxLDL) as previously reported.³⁴ OxLDL contained 4.2–7.4 nmol of TBARS (thiobarbituric acid – reactive substances)/ μ g apoB. Relative electrophoretic mobility (REM) and 2,4,6-trinitrobenzenesulfonic acid (TNBS) reactive amino groups were 1.2–1.3 times and 85–92% of native LDL, respectively.

Nuclear and cytosolic fractionation. Cells were washed once with PBS and lysed in a buffer containing 10 mM HEPES, 1.5 mM MgCl₂, 10 mM KCl, 0.5 mM EDTA, 0.5 mM EDGA, proteases inhibitors, 0.1% Nonidet P-40 pH 7.9 for 10 min on ice and homogenates were centrifuged at 800 \times g at 4 °C for 10 min. The supernatant that contains the cytoplasmic fraction was transferred and saved for western blotting analysis. The nuclear pellet was resuspended in extraction buffer containing 20 mM HEPES, 1.5 mM MgCl₂, 0.2 mM EDTA, 100 mM NaCl, 26% glycerol (v/v), pH 7.9 for 30 min on ice with vortexing at 10-min intervals. Homogenates were centrifuged for 30 min at 14 000 \times g at 4 °C and the supernatant that contains the nuclear fraction was transferred and saved for western blotting analysis.

Western blot analysis. Cells were lysed in solubilizing buffer (10 mM Tris pH 7.4, 150 mM NaCl, 1% Triton X-100, 1% sodium deoxycholate, 0.1% sodium dodecyl sulfate, 1 mM sodium orthovanadate, 1 mM sodium pyrophosphate, 5 mM sodium fluoride, 1 mM phenylmethylsulfonyl fluoride, 1 μ g/ml leupeptin, 1 μ g/ml aprotinin) for 30 min on ice. In all, 40 μ g of protein cell extracts were resolved by SDS-polyacrylamide gel electrophoresis, transferred onto PVDF membranes (Millipore). Then membranes were probed with the indicated primary antibodies and revealed with the secondary antibodies coupled to horseradish peroxidase using the ECL chemoluminescence kit. Membranes were then stripped and reprobed with anti- β -actin antibody to control equal loading of proteins.

Evaluation of cytotoxicity, necrosis and apoptosis. For cytotoxicity experiments, cells were serum starved for 24 h and stimulated for the indicated times at 37 °C. Cytotoxicity was evaluated using the MTT (3-(4,5-dimethylthiazol-2-yl)-2,5-diphenyltetrazolium bromide) test, as previously used.⁷ This method is

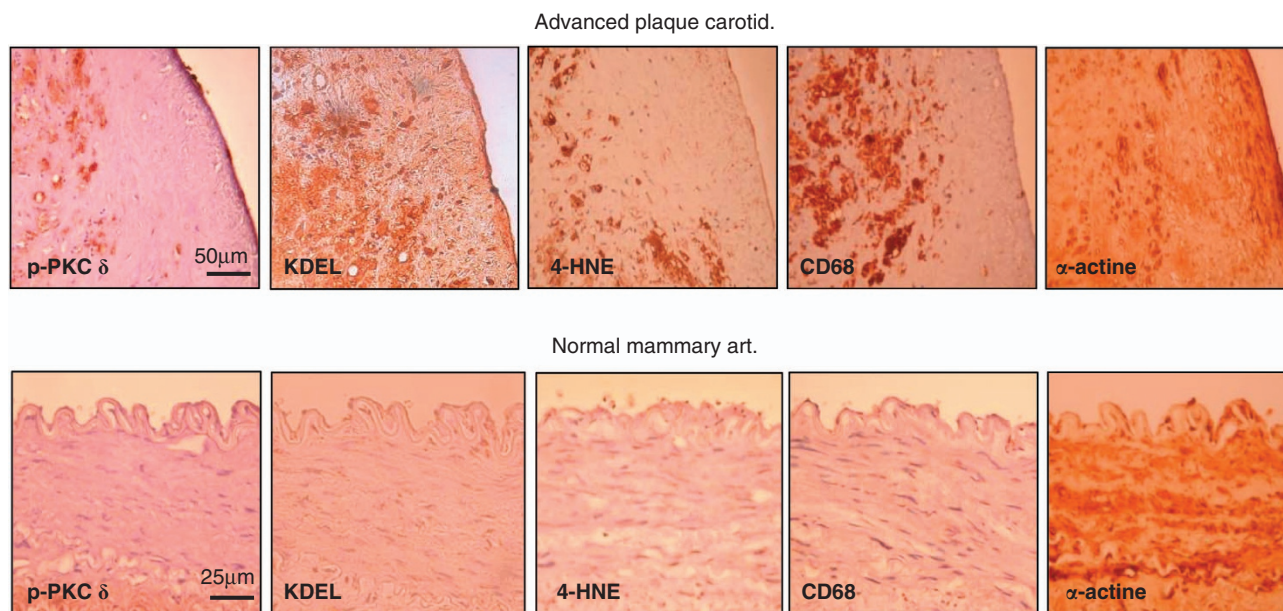


Figure 8 PKC δ colocalized with ER stress and lipid peroxidation markers in advanced human carotid plaques. Immunostaining of human carotid plaque specimens (upper panel) and normal mammary arteries (lower panel) with anti-phosphotyrosine 311 PKC δ , anti-KDEL, anti-4-HNE-adduct, anti-CD68 and anti- α -actin antibodies. The scale bars represent 50 μ m (advanced carotid plaque) and 25 μ m (normal mammary artery)

based on MTT reduction by the respiratory chain and other electron transport systems leading to form non-water-soluble violet formazan crystals that can be determined spectrophotometrically (OD measured at 570 nm) and serves as an estimate for the metabolic activity of living cells. Apoptotic and necrotic cells were counted after fluorescent staining by two fluorescent dyes, the permeant DNA intercalating green fluorescent probe SYTO-13 (0.6 μ M) and the non-permeant DNA intercalating red fluorescent probe propidium iodide (15 μ M) using an inverted fluorescence microscope (Fluovert FU, Leitz, Grand rapids, MI, USA) as previously described.⁷ Normal nuclei exhibit a loose green-colored chromatin. Nuclei of primary necrotic cells exhibit loose red-colored chromatin. Apoptotic nuclei exhibited condensed yellow/green-colored chromatin associated with nucleus fragmentation, whereas post-apoptotic necrotic cells exhibited the same morphological features, but were red-colored.

siRNA transfection. The selected siRNA specific to human PKC δ were ON-TARGET plus SMART pool siRNA human PKC δ (Dharmacon, Waltham, MA, USA). siRNAs were transfected using the Hiperfect reagent (Quiagen, Courtaboeuf, France) according to the manufacturer's recommendations.

Immunofluorescence. Human VSMC grown on cover glass slides were washed with PBS and fixed in PBS/4% paraformaldehyde for 10 min. After blocking with PBS containing 3% BSA for 30 min, cells were incubated with the indicated antibodies for 1 h and revealed with Alexa Fluor 488-conjugated secondary antibody for 1 h. The slides were visualized using a Zeiss LSM 510 fluorescence confocal microscope (Le Pecq, France).

Quantification of intracellular ROS. The generation of intracellular ROS was estimated using the 6-carboxy-2',7'-dichlorodihydrofluorescein diacetate (H₂DCFDA) ROS-sensitive fluorescent probe (5 μ M). Stimulated cells were incubated with the probe 30 min before determination as described.²¹

Immunohistochemistry. Human advanced carotid plaques (patients 70–75 years old) were obtained after endarterectomy (Cardiovascular Surgery Department, CHU Toulouse, France), internal mammary arteries were obtained from patients undergoing coronary artery bypass grafting. Tissues were fixed in formalin and paraffin embedded. Serial 3 μ m thin sections were incubated with the anti-phosphotyrosine 311 PKC δ anti-KDEL, anti-4-HNE-adduct, anti-CD68 and anti- α -actin antibodies, then with appropriate biotin-labeled antibodies, and revealed by using avidin–biotin horseradish peroxidase visualization system (Vectastain, ABC kit Elite, Vector Laboratories, Burlingame, CA, USA). All

experiments were conformed to the declaration of Helsinki in compliance with French legislation and written informed consent was obtained from patients for the use of surgery residual tissue for research.

Statistical analysis. Data are given as mean \pm S.E.M. Statistical comparison of the data was performed using the *t*-test for comparison between two groups and is explained in the figure legends (Sigma stat software, San Jose, CA, USA). Values of $P < 0.05$ were considered statistically significant.

Conflict of Interest

The authors declare no conflict of interest.

Acknowledgements. We thank JC Thiers, C Fouré, A Matassa-Ohm for excellent technical help and Dr. V Gallet (SNCF Laboratory, Toulouse, France) for providing human serum. We are grateful to Dr. F Lezoualc'h for critical reading of the manuscript. These studies were supported by grants from INSERM and Toulouse 3 University to INSERM U1048 team 10.

- Steinberg D, Parthasarathy S, Carew TE, Khoo JC, Witztum JL. Beyond cholesterol. Modifications of low-density lipoprotein that increase its atherogenicity. *N Engl J Med* 1989; **320**: 915–924.
- Napoli C. Oxidation of LDL, atherogenesis, and apoptosis. *Ann NY Acad Sci* 2003; **1010**: 698–709.
- Salvayre R, Auge N, Benoist H, Negre-Salvayre A. Oxidized low-density lipoprotein-induced apoptosis. *Biochim Biophys Acta* 2002; **1585**: 213–221.
- Clarke MC, Figg N, Maguire JJ, Davenport AP, Goddard M, Littlewood TD *et al*. Apoptosis of vascular smooth muscle cells induces features of plaque vulnerability in atherosclerosis. *Nat Med* 2006; **12**: 1075–1080.
- Ingueneau C, Huynh-Do U, Thiers JC, Negre-Salvayre A, Salvayre R, Vindis C. Caveolin-1 sensitizes vascular smooth muscle cells to mildly oxidized LDL-induced apoptosis. *Biochem Biophys Res Commun* 2008; **369**: 889–893.
- Ingueneau C, Huynh UD, Marcheix B, Athias A, Gamber P, Negre-Salvayre A *et al*. TRPC1 is regulated by caveolin-1 and is involved in oxidized LDL-induced apoptosis of vascular smooth muscle cells. *J Cell Mol Med* 2009; **13**: 1620–1631.
- Muller C, Salvayre R, Negre-Salvayre A, Vindis C. HDLs inhibit endoplasmic reticulum stress and autophagic response induced by oxidized LDLs. *Cell Death Differ* 2011; **18**: 817–828.
- Zhang K, Kaufman RJ. From endoplasmic-reticulum stress to the inflammatory response. *Nature* 2008; **454**: 455–462.

9. Marciniak SJ, Yun CY, Oyamomari S, Novoa I, Zhang Y, Jungreis R *et al*. CHOP induces death by promoting protein synthesis and oxidation in the stressed endoplasmic reticulum. *Genes Dev* 2004; **18**: 3066–3077.
10. McCullough KD, Martindale JL, Klotz LO, Aw TY, Holbrook NJ. Gadd153 sensitizes cells to endoplasmic reticulum stress by down-regulating Bcl2 and perturbing the cellular redox state. *Mol Cell Biol* 2001; **21**: 1249–1259.
11. Sanson M, Auge N, Vindis C, Muller C, Bando Y, Thiers JC *et al*. Oxidized low-density lipoproteins trigger endoplasmic reticulum stress in vascular cells prevention by oxygen-regulated protein 150 expression. *Circ Res* 2009; **104**: 328–U102.
12. Myoishi M, Hao H, Minamino T, Watanabe K, Nishihira K, Hatakeyama K *et al*. Increased endoplasmic reticulum stress in atherosclerotic plaques associated with acute coronary syndrome. *Circulation* 2007; **116**: 1226–1233.
13. Reyland ME. Protein kinase Cdelta and apoptosis. *Biochem Soc Trans* 2007; **35**: 1001–1004.
14. Leitges M, Mayr M, Braun U, Mayr U, Li C, Pfister G *et al*. Exacerbated vein graft arteriosclerosis in protein kinase Cdelta-null mice. *J Clin Invest* 2001; **108**: 1505–1512.
15. Yamanouchi D, Kato K, Ryer EJ, Zhang F, Liu B. Protein kinase C delta mediates arterial injury responses through regulation of vascular smooth muscle cell apoptosis. *Cardiovasc Res* 2010; **85**: 434–443.
16. Greene MW, Ruhoff MS, Burrington CM, Garofalo RS, Orena SJ. TNFalpha activation of PKCdelta, mediated by NFkappaB and ER stress, cross-talks with the insulin signaling cascade. *Cell Signal* 2010; **22**: 274–284.
17. Yang H, Chen S, Tang Y, Dai Y. Interleukin-10 down-regulates oxLDL induced expression of scavenger receptor A and Bak-1 in macrophages derived from THP-1 cells. *Arch Biochem Biophys* 2011; **512**: 30–37.
18. Konishi H, Yamauchi E, Taniguchi H, Yamamoto T, Matsuzaki H, Takemura Y *et al*. Phosphorylation sites of protein kinase C delta in H₂O₂-treated cells and its activation by tyrosine kinase in vitro. *Proc Natl Acad Sci USA* 2001; **98**: 6587–6592.
19. Kato K, Yamanouchi D, Esbona K, Kamiya K, Zhang F, Kent KC *et al*. Caspase-mediated protein kinase C-delta cleavage is necessary for apoptosis of vascular smooth muscle cells. *Am J Physiol Heart Circ Physiol* 2009; **297**: H2253–H2261.
20. Bouguerne B, Belkheiri N, Bedos-Belval F, Vindis C, Uchida K, Duran H *et al*. Antiatherogenic effect of bisvanillyl-hydralazone, a new hydralazine derivative with antioxidant, carbonyl scavenger, and antiapoptotic properties. *Antioxid Redox Signal* 2011; **14**: 2093–2106.
21. Robbesyn F, Garcia V, Auge N, Vieira O, Frisach MF, Salvayre R *et al*. HDL counterbalance the proinflammatory effect of oxidized LDL by inhibiting intracellular reactive oxygen species rise, proteasome activation, and subsequent NF-kappaB activation in smooth muscle cells. *FASEB J* 2003; **17**: 743–745.
22. Beckman JS, Minor RL Jr., White CW, Repine JE, Rosen GM, Freeman BA. Superoxide dismutase and catalase conjugated to polyethylene glycol increases endothelial enzyme activity and oxidant resistance. *J Biol Chem* 1988; **263**: 6884–6892.
23. Qi X, Mochly-Rosen D. The PKCdelta-Abl complex communicates ER stress to the mitochondria—an essential step in subsequent apoptosis. *J Cell Sci* 2008; **121** (Pt 6): 804–813.
24. Chiu SC, Chen SP, Huang SY, Wang MJ, Lin SZ, Harn HJ *et al*. Induction of apoptosis coupled to endoplasmic reticulum stress in human prostate cancer cells by n-butylideneephthalide. *PLoS One* 2012; **7**: e33742.
25. Reyland ME. Protein kinase C isoforms: multi-functional regulators of cell life and death. *Front Biosci* 2009; **14**: 2386–2399.
26. Liu B, Ryer EJ, Kundi R, Kamiya K, Itoh H, Faries PL *et al*. Protein kinase C-delta regulates migration and proliferation of vascular smooth muscle cells through the extracellular signal-regulated kinase 1/2. *J Vasc Surg* 2007; **45**: 160–168.
27. Altenhofer S, Kleikers PW, Radermacher KA, Scheurer P, Rob Hermans JJ, Schifers P *et al*. The NOX toolbox: validating the role of NADPH oxidases in physiology and disease. *Cell Mol Life Sci* 2012; **69**: 2327–2343.
28. Stielow C, Catar RA, Muller G, Wingle K, Scheurer P, Schmidt HH *et al*. Novel Nox inhibitor of oxLDL-induced reactive oxygen species formation in human endothelial cells. *Biochem Biophys Res Commun* 2006; **344**: 200–205.
29. Brodie C, Blumberg PM. Regulation of cell apoptosis by protein kinase c delta. *Apoptosis* 2003; **8**: 19–27.
30. DeVries TA, Neville MC, Reyland ME. Nuclear import of PKCdelta is required for apoptosis: identification of a novel nuclear import sequence. *EMBO J* 2002; **21**: 6050–6060.
31. Fujii T, Garcia-Bermejo ML, Bernabo JL, Caamano J, Ohba M, Kuroki T *et al*. Involvement of protein kinase C delta (PKCdelta) in phorbol ester-induced apoptosis in LNCaP prostate cancer cells. Lack of proteolytic cleavage of PKCdelta. *J Biol Chem* 2000; **275**: 7574–7582.
32. Galvani S, Trayssac M, Auge N, Thiers JC, Calise D, Krell HW *et al*. A key role for matrix metalloproteinases and neutral sphingomyelinase-2 in transplant vasculopathy triggered by anti-HLA antibody. *Circulation* 2011; **124**: 2725–2734.
33. Humphries MJ, Limesand KH, Schneider JC, Nakayama KI, Anderson SM, Reyland ME. Suppression of apoptosis in the protein kinase Cdelta null mouse in vivo. *J Biol Chem* 2006; **281**: 9728–9737.
34. Vindis C, Elbaz M, Escargueil-Blanc I, Auge N, Henriquez A, Thiers JC *et al*. Two distinct calcium-dependent mitochondrial pathways are involved in oxidized LDL-induced apoptosis. *Arterioscler Thromb Vasc Biol* 2005; **25**: 639–645.



Cell Death and Disease is an open-access journal published by Nature Publishing Group. This work is licensed under the Creative Commons Attribution-NonCommercial-No Derivative Works 3.0 Unported License. To view a copy of this license, visit <http://creativecommons.org/licenses/by-nc-nd/3.0/>

Supplementary Information accompanies this paper on Cell Death and Disease website (<http://www.nature.com/cddis>)